Regional climate effects of Arctic Haze

A. Rinke, K. Dethloff, and M. Fortmann

Alfred Wegener Institute for Polar and Marine Research, Potsdam, Germany

Received 21 April 2004; revised 7 June 2004; accepted 16 July 2004; published 17 August 2004.

[1] The direct climate effect of aerosols has been studied within a regional atmospheric model of the Arctic. The mean springtime effect on the near surface temperature has been estimated and showed to be within ±1 K. However, the aerosol effect varies strongly regionally depending on the surface albedo, atmospheric humidity, and cloud condition of the region. The interannual variability of the aerosol effect is very pronounced (for the near surface temperature in the order of 2 K) and is connected with the strong varying year-specific atmospheric conditions. Due to the high horizontal resolution of the model, it was possible to assess the influence both on the large-scale as well as on the meso-scale atmospheric circulation. Through the aerosol-radiation-circulation feedback, the scattering and absorption of radiation by aerosol cause pressure pattern changes which have the potential to modify Arctic teleconnection patterns like the Barents Sea Oscillation. *INDEX TERMS:* 3329 Meteorology and Atmospheric Dynamics: Mesoscale meteorology; 3337 Meteorology and Atmospheric Dynamics: Numerical modeling and data assimilation; 3349 Meteorology and Atmospheric Dynamics: Polar meteorology; 3359 Meteorology and Atmospheric Dynamics: Radiative processes. **Citation:** Rinke, A., K. Dethloff, and M. Fortmann (2004), Regional climate effects of Arctic Haze, *Geophys. Res. Lett.*, *31*, L16202, doi:10.1029/2004GL020318.

1. Introduction

[2] On one side, the estimates for future climate show the largest warming signal over the Arctic region. On the other side, the magnitudes of both the direct and indirect aerosol effects are largely unknown and therefore the tropospheric aerosols are one of the key uncertainty parameters in climate change estimates [*Houghton et al.*, 2001]. During winter and spring seasons, the long-range transport of anthropogenic pollution leads to enhanced aerosol concentrations in the Arctic troposphere, known as the Arctic Haze phenomenon [e.g., *Heintzenberg*, 1989; *Shaw*, 1995]. Beside the predominant sulphate particles which cool the surface, soot (containing black carbon) occurs with substantial concentrations. The latter absorbs solar radiation and may warm climate, although this effect could be small or even negative, taking into account the altitude of injection of the aerosols [*Penner et al.*, 2003]. Investigations with a global climate model [*Blanchet*, 1989] indicated a regionally strong varying surface warming in the high Arctic of 1 to 2 K. The interaction among aerosols, clouds, and climate conditions is of particular complexity in the Arctic because of the high surface albedo; the marked annual cycle of Arctic aerosol characteristics; the extreme static stability of Arctic lower troposphere; the sensitivity of ice nucleation to aerosols; the complex radiative interactions between aerosols, clouds, and sea ice; and the annual cycle of aerosol residence time in the Arctic [*Curry*, 1995].

[3] Arctic Haze is a phenomenon with a strong regional signature because of its strong temporally and spatially varying distribution. Therefore, the use of high resolution regional atmospheric models covering the Arctic is highly recommended for studying its climatic impacts. The regional models have a typical horizontal resolution of 20–50 km and are of the same complexity concerning the physical processes taken into account as the global climate models. The absence of a complete and consistent Arctic aerosol data sets anticipates a realistic estimation of the Arctic Haze climatic effect.

2. Model and Simulations

[4] The regional atmospheric climate model employed in this study is called HIRHAM and has been applied to a variety of Arctic climate studies. The integration domain covers the whole Arctic north of about 60°N with a horizontal resolution of 0.5 degrees. The vertical discretization consists of 19 irregularly spaced levels. The model is forced at the lateral boundaries using temperature, wind, humidity, and surface pressure (updated every 6 hours) and at the lower boundary using sea surface temperature and sea ice fraction (updated daily) provided from operational analyses from the European Centre for Medium-Range Weather Forecasts.

[5] HIRHAM uses the physical parameterization package of the ECHAM4 atmospheric general circulation model [*Roeckner et al.*, 1996]. ECHAM4 incorporates the modified Morcrette radiative scheme with an explicit treatment of the radiative effects of cloud droplets (water and ice) and aerosol particles (direct effect) [*Morcrette*, 1991]. The aerosol data used here are taken from the Global Aerosol Data Set (GADS) [*Koepke et al.*, 1997] (http://www.lrz-muenchen.de/~uh234an/www/radaer/gads.html). Using the GADS, the aerosol has been incorporated by using a prescribed climatology. The GADS provides aerosol microphysical and optical parameters of 10 main aerosol components and the aerosol radiative properties (optical thickness, single-scattering albedo, asymmetry parameter) are computed by taking into account the effect of relative humidity.

[6] The Arctic Haze aerosol has been described as a mixture of three GADS aerosol components: WASO (water soluble sulphate, nitrate), SOOT (organic and black carbon) and SSAM (sea salt particles with radii between 0.1–1 μm). Numerous measurements performed in the Arctic have shown that these are the main components of Arctic Haze. The aerosol optical parameters of the mixture are given by

0094-8276/04/2004GL020318$05.00

(a) mean effect on 2-m air temperature

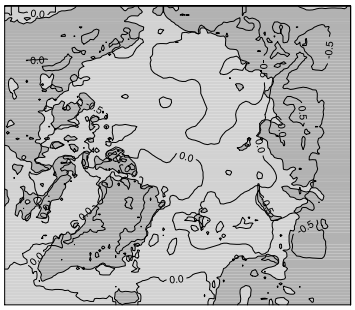

(b) mean effect on mean sea level pressure

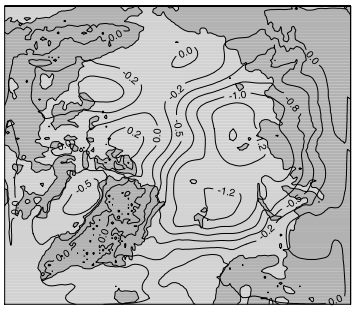

Figure 1. Ensemble mean aerosol effect on (a) the 2-m air temperature [K] and (b) the mean sea level pressure [hPa] for March (ensemble 1989–95). See color version of this figure in the HTML.

R. Treffeisen (manuscript in preparation, 2004). The aerosol was placed between the model levels 14–17 corresponding to heights of 400–2000 m.

[7] The simulations have been performed for a March ensemble of the years 1989–1995. The multiplicity in the atmospheric circulation of this ensemble reflects a significant fraction of the observed interannual springtime variability and thus permits an examination of the aerosol effect under a wide range of conditions, including the representation of its interannual variability. The model has been run twice over this ensemble, once without any aerosol (''control run''), and once with aerosol included (''aerosol run''). The aerosol effect has been calculated as the difference between the aerosol and the control runs.

3. Results

[8] The study evaluates the direct climatic effect of aerosol, and its impact on the temperature (as a measure of the radiative balance) as well as on the circulation patterns is presented here. Figure 1a shows the ensemble mean aerosol effect on the 2-m air temperature. The most striking feature is the strong regionally varying mesoscale pattern of the aerosol effect ranging from a cooling to a warming within the order of ±1 K. The strongest warming is found in the area between Spitsbergen, Barents and Kara Seas, and Taimyr Peninsula. The strongest cooling appears over the East Siberian Sea and the Canadian Archipelago. The mean cooling in the near surface layers is opposite to a warming within the aerosol layer and indicates a change of the atmospheric stability (amplifying of prevalent near surface inversions). The changed (damped) vertical exchange processes of turbulent fluxes of momentum, heat, and water contribute to the change of the circulation patterns as described in *Dethloff et al.* [2001]. Figure 1b shows that the mean sea level pressure (SLP) is reduced by up to 2 hPa in the Kara- and Laptev Seas and demonstrates an expansion of the through connected with the Islandic low. This pressure reduction extends up to the free troposphere (~15 gpm reduction of the 500 hPa height). The direct aerosol effect influences not only the radiative fluxes but also the dynamical variables via the nonlinear interactions within the model. The most important interaction is the aerosol-radiation-circulation-feedback: The direct aerosol radiative forcing in the vertical column of each of the model grid cells leads to diabatic heating rate profile changes which modify the vertical structure of the thermodynamic variables and the atmospheric dynamic structure. These modifications affect cloud properties (cloud fraction, optical depth) which in turn modify the radiative fluxes which feed back to the dynamics. The temperature profile changes influence the longwave radiative flux profiles and the clouds are linked with synoptic scale systems. The resulting modification of the synoptic circulation patterns is demonstrated in the next paragraph for one example. The changed humidity/cloud structures modify in turn the aerosol optical depth closing this feedback loop. It is worth noting that the primary aerosol effect on the surface radiation budget is combined with a major part felt within the troposphere.

[9] Figure 2 shows as one example the aerosol effect for a specific year. The mean circulation in spring 1990 was characterized by a northerly wide-stretched low pressure system with the center in the Kara Sea and thus shows an anomalous March atmospheric circulation pattern connected with observed record reductions in Arctic sea ice cover in 1990 [*Serreze et al.*, 1995]. Under these circumstances, the aerosol effect on the temperature (Figure 2a) ranges between −3 K and +3 K and warms the eastern Arctic while it cools the western Arctic. The main low-pressure system over the Kara Sea is weakened by 3 hPa (Figure 2b) and the geopotential height pattern changes are of barotropic nature (weakening through the atmospheric column and attenuation of the vortex; at 500 hPa decrease by 50 gpm). The mean aerosol effect for this year has a different structure and is about three times stronger than the climatological mean effect. That the synoptic-scale cyclones change significantly when aerosol effects are included is demonstrated in the following figures. Figure 2c shows the different evolution of the SLP fields obtained for the control and the aerosol runs after 20 days. We recognize the different formation of synoptic-scale circulation via baroclinic instability changes due to the aerosol starting remarkably after 12 days. Such changes have large implications as baroclinic eddies are the primary agents of temperature, humidity and momentum transport in the atmosphere. The interdiurnal variability of SLP (absolute day-to- day changes within a month) serves as a measure for the baroclinicity and its change due to the aerosol is presented in Figure 2d. It has been calculated for the control and aerosol runs, averaged over the month, and subtracted. It is demonstrated that the direct aerosol effects regionally modify (increase or decrease) the mean atmospheric baroclinicity.

[10] The strength of the calculated aerosol effect depends strongly on the effective absorption of solar radiation by

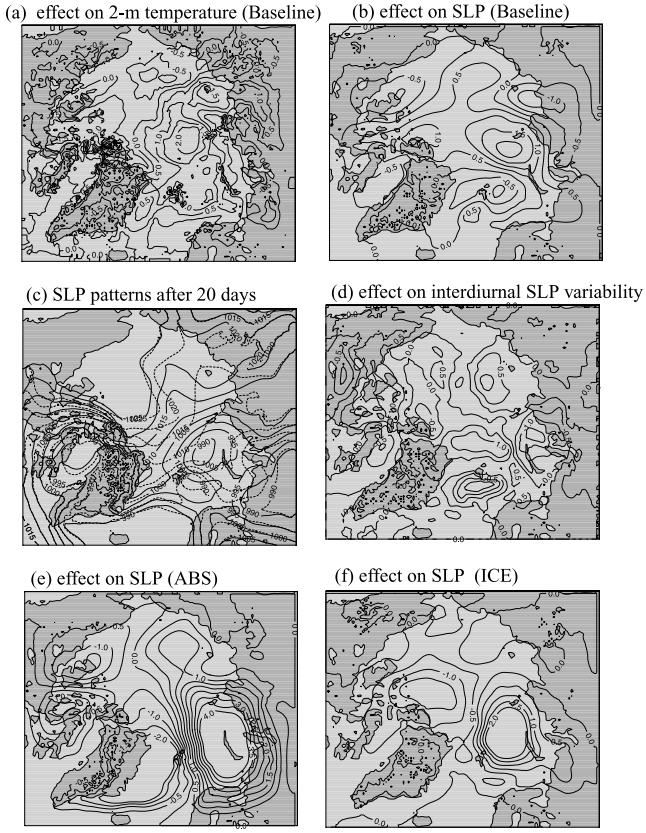

Figure 2. Aerosol effect on the 2-m air temperature and the mean sea level pressure (SLP) for March 1990. For the baseline simulation (a, b). The SLP fields after 20 days simulation time for the control (solid lines) and the aerosol run (dashed lines) (c). The effect on the interdiurnal SLP variability (d). The effect on SLP for sensitivity runs: (e) run with increased aerosol absorption (ABS), (f) run with changed ice cloud parameterization (ICE). SLP in [hPa] and temperature in [K]. See color version of this figure in the HTML.

black carbon. But, the literature gives a wide range for the specific black carbon absorption (absorption cross section for a given carbon particle divided by mass) of 3–25 m^2/g and can be explained by the physical and chemical variability of soot related to the combustion and the degree of atmospheric aging [*Liousse et al.*, 1993; *Schnaiter et al.*, 2003]. The GADS uses 8.6 m^2/g for its soot component lying more in the lower part of this range. Soot aerosol occurs internally mixed with sulphate and other water-soluble particles [*Hara et al.*, 2003]. The GADS does not take this into account, but this process would have large implications (increase) for the WASO absorption cross section. To investigate these uncertainties, the simulations have been repeated with increased (by 10%) absorption cross sections (the extinction is held unaffected). The aerosol absorption of solar radiation is increased by ~20%. The aerosol effect on the temperature is amplified, within ±6 K and shows a main warming over the Barents and Kara Seas. Figure 2e shows the implication for the aerosol effect on the SLP. A pronounced pattern with increased pressure over the Barents and Kara Seas and decreased pressure over the Fram Strait with up to 6 hPa changes is seen. This pattern is well known as the Barents Sea Oscillation [*Skeie*, 2000] and shows that the direct aerosol effect has the potential to change the mode and/or the strength of this large-scale teleconnection pattern. Due to the strong aerosol-radiation-cloud-circulation feedbacks, it has to be investigated if the applied specific cloud parameterization affects the calculated direct aerosol effect. For this purpose, the ice cloud parameterization used in HIRHAM [*Rockel et al.*, 1991] was replaced with those of *Ebert and Curry* [1992]. Both parameterizations describe the ice cloud optical properties in terms of the effective radius of the ice crystal size distribution and the ice water path, but are based on different assumptions about the ice particle shape and size distribution. As presented in Figure 2f, the aerosol effect changed remarkably due to the different cloud parameterization. The magnitude of the effects is of comparable order as before, but the regional patterns of the aerosol effect changed dramatically. The temperature pattern shows a warming over the western Arctic and cooling of the Eastern Arctic which is completely reverse to Figure 2a. The SLP effect shows a wave number 1 pattern with a weakening of both the Kara Sea low and the Beaufort Sea/Canadian Basin high with potential implications for the sea ice drift.

[11] To characterize the interannual variability of the aerosol effect, the ensemble standard deviation has been calculated. A small value indicates agreement in the calculated aerosol effect among the individual simulations of different years and therefore a low interannual variability, while a large value indicates disagreement in the simulations and a high variability. Figure 3 shows those of the 2-m air temperature and SLP. The year-to-year variability of the aerosol effect is very pronounced and large. The temperature variability can reach up to 2 K so that it is twice as large as

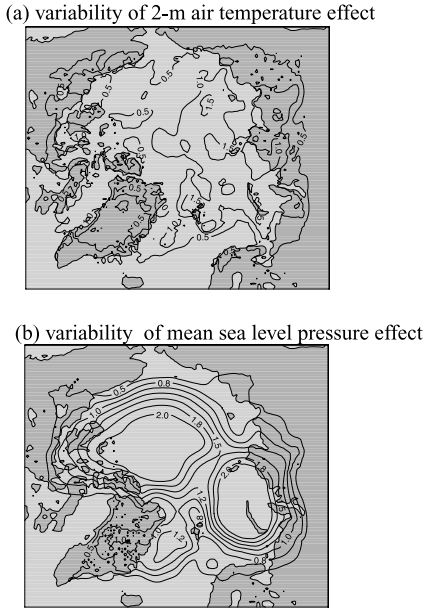

Figure 3. Ensemble standard deviation (year-to-year variability) of the aerosol effect on (a) the 2-m air temperature [K] and (b) the mean sea level pressure [hPa] for March (ensemble 1989–95). See color version of this figure in the HTML.

the mean effect. The SLP variability is up to 3 hPa (which is of about the same order as the mean effect) and shows a pronounced wave 2 pattern with maximum variability over the Kara and Beaufort Seas. The large interannual variability of the aerosol effect is explained by the strong synoptic variability (different circulation patterns in different March [*Rinke et al.*, 1999]) which is connected with pronounced regional surface weather changes. Especially changes of the air humidity, clouds, and surface albedo contribute to significant changes of the magnitude and sign of the aerosol effect due to the aerosol-radiation- circulation-feedbacks.

4. Conclusions

[12] Arctic Haze exerts a not negligible climate effect; a pronounced regionally varying cooling and warming have been calculated. The magnitude and the regional pattern of the direct aerosol effect have been shown to depend on the assumed aerosol absorption and the specified model's ice cloud optical properties. The distinctive interannual variability of the aerosol effect is largely driven by the year-specific atmospheric conditions, but the identification of the origin of the year-to-year variability needs further investigations to get substantial advance in the current knowledge.

[13] Although only the direct aerosol effect has been taken into account, the aerosols strongly modify the regional circulation patterns and humidity/cloud structures, i.e., besides the local thermodynamic impacts, there are significant regional dynamical responses to the aerosol forcing. It was shown that the direct aerosol effect has the potential to change the mode and/or the strength of large-scale atmospheric teleconnection patterns, like the Barents Sea Oscillation. They are associated with the interannual and decadal variability of Arctic climate processes which has strong implications for the climate development of Europe.

[14] **Acknowledgment.** This research has been funded by the European Union project GLIMPSE (EVK2-CT-2002-00164).

References

Blanchet, J.-P. (1989), Toward estimation of climatic effects due to arctic aerosol, *Atmos. Environ.*, *23*, 2609–2625.

Curry, J. A. (1995), Interactions among aerosols, clouds, and climate of the Arctic Ocean, *Sci. Total Environ.*, *160/161*, 777–791.

Dethloff, K., C. Abegg, A. Rinke, I. Hebestad, and V. Romanov (2001), Sensitivity of Arctic climate simulations to different boundary layer parameterizations in a regional climate model, *Tellus, Ser. A*, *53*, 1–26.

Ebert, E. E., and J. A. Curry (1992), A parameterization of ice cloud optical properties for climate models, *J. Geophys. Res.*, *97*, 3831–3836.

Hara, K., S. Yamagata, T. Yamanouchi, K. Sato, A. Herber, Y. Iwasaka, M. Nagatani, and A. Nakada (2003), Mixing states of individual aerosol particles in spring Arctic troposphere during ASTAR 2000 campaign, *J. Geophys. Res.*, *108*(D7), 4209, doi:10.1029/2002JD002513.

Heintzenberg, J. (1989), Arctic Haze: Air pollution in polar regions, *Ambio*, *18*, 50–55.

Houghton, J. T., et al. (2001), *Climate Change 2001: The Scientific Basis: Contribution of Working Group I to the third assessment report of the Intergovernmental Panel on Climate Change*, Cambridge Univ. Press, New York.

Koepke, P., M. Heß, I. Schult, and E. P. Shettle (1997), Global aerosol data set, *MPI Rep. 243*, 44 pp., Max Planck Inst. for Meteorol., Hamburg, Germany.

Liousse, C., H. Chachier, and S. G. Jennings (1993), Optical and thermal measurements of black carbon aerosol content in different environment, *Atmos. Environ.*, *27*, 1203–1211.

Morcrette, J.-J. (1991), Radiation and cloud radiative cloud properties in the European Centre for Medium Range Weather Forecasts forecasting system, *J. Geophys. Res.*, *96*, 9121–9132.

Penner, J. E., S. Y. Zhang, and C. C. Chuang (2003), Soot and smoke aerosol may not warm climate, *J. Geophys. Res.*, *108*(D21), 4657, doi:10.1029/2003JD003409.

Rinke, A., K. Dethloff, and J. H. Christensen (1999), Arctic winter climate and its interannual variations simulated by a regional climate model, *J. Geophys. Res.*, *104*, 19,027–19,038.

Rockel, B., E. Raschke, and B. Weyres (1991), A parameterization of broad band radiative transfer properties of water, ice and mixed clouds, *Beitr. Phys. Atmos.*, *64*, 1–12.

Roeckner, E., et al. (1996), The atmospheric general circulation model ECHAM-4: Model description and simulation of present-day climate, *Rep. 218*, 90 pp., Max Planck Inst. for Meteorol., Hamburg, Germany.

Schnaiter, M., H. Horvath, O. Moehler, K. H. Naumann, H. Saathoff, and O. W. Schoeck (2003), UV-VIS-NIR spectral optical properties of soot and soot containing aerosols, *Aerosol Sci.*, *34*, 1421–1444.

Serreze, M. C., J. A. Maslanik, J. R. Key, and R. F. Kokaly (1995), Diagnosis of the record minimum in Arctic sea ice area during 1990 and associated snow cover extremes, *Geophys. Res. Lett.*, *22*, 2183–2186.

Shaw, G. E. (1995), The Arctic haze phenomenon, *Bull. Am. Meteorol. Soc.*, *76*, 2403–2412.

Skeie, P. (2000), Meridional flow variability over the Nordic seas in the Arctic Oscillation framework, *Geophys. Res. Lett.*, *27*, 2569–2572.

K. Dethloff, M. Fortmann, and A. Rinke, Alfred Wegener Institute for Polar and Marine Research, Telegrafenberg A43, D-14473 Potsdam, Germany. (arinke@awi-potsdam.de)